

Supplementary Appendix

This appendix has been provided by the authors to give readers additional information about their work.

Supplement to: Boyden SE, Desai A, Cruse G, et al. Vibratory urticaria associated with a missense variant in *ADGRE2*. *N Engl J Med* 2016;374:656-63. DOI: 10.1056/NEJMoa1500611

TABLE OF CONTENTS

I. Supplementary Methods	3-13
II. Supplementary Figures	
1. Serum tryptase levels in response to vibration	14
2. Candidate interval on chromosome 19p13 defined by linkage scans	15
3. Expression of ADGRE2 in mast cells	16-18
4. Expression, cleavage, adhesion, and trafficking of mutant ADGRE2	19-24
III. Supplementary Tables	
1. Variant databases in which <i>ADGRE2</i> :c.1475G>A is absent	25
2. Physical urticaria patients screened for <i>ADGRE2</i> variants	26
3. Pairwise <i>P</i> values for constitutive degranulation of LAD2 cells	27
4. Pairwise <i>P</i> values for vibration-induced degranulation of LAD2 cells	28
IV. Supplementary References	29

I. Supplementary Methods

Patient ascertainment

Families 1 and 3 were enrolled and evaluated at the National Institutes of Health Clinical Center under a protocol approved by the Institutional Review Board of the National Institute of Allergy and Infectious Diseases. Family 2 was enrolled at Yale University as previously described.¹ All subjects provided written informed consent.

Forearm vortex challenge and serum histamine and tryptase release

To elicit vibratory urticaria symptoms in a clinical setting, the anterior forearm of a subject was placed horizontally on the 3 inch platform of a laboratory vortex for a 4 minute challenge at 2500 rpm. The skin reaction was observed at the challenge site at baseline and sequentially following the challenge for 60 minutes. Systemic symptoms were also documented during this time period. Serum histamine levels from serial blood draws during the 60 minute postchallenge period were measured using a competitive enzyme immunoassay (SPI-Bio). Serum tryptase levels from the same time points were measured using the ImmunoCAP 100 system (Phadia).

Immunohistochemical staining

Tissues were fixed in 10% neutral buffered formalin, routinely processed, embedded in paraffin, and sectioned at 5 μ m. Immunohistochemistry was performed using the Discovery XT instrument with RedMap detection kit (Ventana Medical Systems), and a monoclonal mouse anti-human mast cell tryptase antibody, (Abcam #2378, clone AA1) at a dilution of 1:100. A

biotinylated goat anti-mouse Super Sensitive Link (BioGenex #HK335-9M) was used undiluted as a secondary antibody. Images were taken at 20X and 60X magnification.

Linkage analysis

Members of Family 2 were initially genotyped at a genomewide panel of short tandem repeat markers (Applied Biosystems), and we later genotyped 10 members of Family 1 and 24 members of Family 2 at 298,563 single nucleotide polymorphisms (SNPs) using the HumanCytoSNP-12 array (Illumina). To rule out sample identity errors, sample genders and relatedness were checked by examining heterozygous call rates on the X chromosome, total call rates on the Y chromosome, Mendelian inheritance error rates, and overall genotype concordance between pairs of individuals. Low-quality and uninformative SNPs were removed, producing a filtered marker panel of 186,940 SNPs for Family 1 and 102,361 SNPs for Family 2. Genomewide multipoint parametric linkage analysis was conducted on the Biowulf Linux compute cluster at NIH, using MERLIN v1.1.2² under an autosomal dominant model. The disease allele frequency was set to 0.0001 and we used a full penetrance, zero phenocopy model. The error checking and Pedwipe functions were used to remove unlikely genotypes. Because of the very large size of Family 2, the -two option in MERLIN was used to allow at most two recombination events between consecutive informative markers, thereby reducing the computational burden of the scan.

Exome sequencing and other genetic analysis

Exome sequencing was performed for all ten available samples from Family 1 (seven affected and three unaffected) at the NIH Intramural Sequencing Center. Exome capture was performed using the TruSeq Exome Enrichment Kit v1 (Illumina) and libraries were sequenced on the

HiSeq 2000 platform (Illumina) using 2 x 100 bp paired-end reads, to an average depth of coverage in the target intervals of 82X across all samples, and with an average of 92% of targeted bases producing high-confidence calls. The data were analyzed using the Biowulf Linux compute cluster at NIH, as follows: per-sample alignment of reads to the Build 37 human reference genome using Novoalign and marking of duplicate reads with Picard, followed by multi-sample re-alignment around small insertions and deletions, re-calibration of per-base quality scores, variant calling with HaplotypeCaller, and re-calibration of variant quality scores using the Genome Analysis Tool Kit (GATK),³ and finally variant annotation with Annovar.⁴ Coverage depth was assessed using Bedtools.⁵ To rule out sample identity errors, sample genders and relatedness were checked as for the linkage scans. Annotated variants were filtered to include only those that met the following criteria: were either nonsynonymous, in a 5' untranslated region, or in splice sites within 6 base pairs of an exon; were absent from dbSNP v129; had less than 0.1% variant allele frequency in 1094 genomes from the 1000 Genomes Project (April 2012 release), 6503 exomes from the NHLBI Exome Sequencing Project, 95 exomes from the NIEHS Environmental Genome Project, 662 exomes from the NHGRI ClinSeq project, and 69 publicly available genomes sequenced at Complete Genomics, Inc.; were within the chromosome 19 minimum consensus linkage interval; and cosegregated with the phenotype among all sequenced family members, allowing for uncalled or miscalled genotypes due to poor coverage (<20X) or quality scores (<30). Putative candidates were then individually examined in the Integrative Genomics Viewer (IGV)⁶ to eliminate probable false-positives arising from low coverage or mis-aligned reads, and passing variants were validated and tested for cosegregation in all available members of all three families by Sanger sequencing.

Polymerase chain reaction (PCR) and Sanger sequencing were performed according to standard protocols. The variant was genotyped in DNA samples from unrelated control subjects using either a Custom TaqMan SNP Genotyping Assay (Applied Biosystems) (852 Lebanese samples), Sanger sequencing (101 Lebanese and 100 Israeli samples), or exome sequencing (152 Lebanese samples).

Cell culture

Stock primary human mast cells (HuMCs) were prepared from frozen CD34⁺ progenitors isolated from peripheral blood of healthy volunteers following G-CSF stimulation and apheresis. Thawed cells were cultured for 7 weeks in StemPro-34 medium (Life Technologies) as previously described,⁷ with 100 ng/mL human recombinant stem cell factor (rSCF) and 100 ng/mL human recombinant IL-6 (PeproTech), plus 30 ng/mL human recombinant IL-3 for the first week only. Primary mast cells (PMCs) were derived from CD34⁺ progenitors isolated from 100 mL untreated fresh peripheral whole blood. Mononuclear cells were obtained after density gradient centrifugation, and a human progenitor cell enrichment kit was used to obtain CD34⁺ cells by negative separation (Stemcell Technologies). Cells were cultured as above.

Mouse bone marrow-derived mast cell (BMMC) progenitors were obtained by femur lavage and cultured for 4-6 weeks in RPMI 1640 medium supplemented with 10% fetal bovine serum, 4 mM glutamine, 100 U/mL penicillin, 100 µg/mL streptomycin, 25 mM HEPES, 1 mM sodium pyruvate, 1% nonessential amino acids, 50 mM β-mercaptoethanol and 30 ng/mL mouse recombinant IL-3 (PeproTech), as described.⁸ During culture of both human and mouse mast cells, expression of KIT and the IgE receptor FcεRI was monitored by flow cytometry to ensure that a population of >95% double-positive mast cells was obtained, as described.^{8,9}

***ADGRE2* expression**

For end-point reverse transcription (RT)-PCR, total RNA was extracted from HMC1.1, HMC1.2, and LAD2¹⁰ human mast cell lines, and primary HuMCs and PMCs from healthy volunteers. Primers spanning the exon 11-12 junction were used to test for *ADGRE2* mRNA expression. For semi-quantitative RT-PCR, mRNA expression was assayed in 18 tissues from the FirstChoice Human Total RNA Survey Panel (Ambion), as well as Human Dorsal Root Ganglion Total RNA (Clontech) and total RNA from human peripheral blood mononuclear cells (PBMCs), HuMCs, and LAD2 cells. SuperScript III First-Strand Synthesis SuperMix (Invitrogen) was used to reverse transcribe cDNA from equal amounts of RNA, and amplicons spanning the exon 11-12 junction from *ADGRE2* and the exon 6-7 junction from the housekeeping gene *RPLP0* were amplified for 30 cycles and subjected to agarose gel electrophoresis.

ADGRE2 surface and total protein expression were assayed by flow cytometry in HMC1.1, HMC1.2, and LAD2 human mast cell lines, and primary HuMCs and PMCs. Cells were washed with 0.1% bovine serum albumin (BSA) in phosphate-buffered saline (PBS), and for total protein detection, cells were then permeabilized by incubating for 30 minutes in 0.1% BSA plus 0.5% saponin in PBS. Fcγ receptors were blocked with Human TruStain FCX (BioLegend). Cells were then stained with biotinylated monoclonal mouse anti-human *ADGRE2* α subunit antibody, clone 2A1¹¹ (AbD Serotec) or polyclonal rabbit anti-human *ADGRE2* β subunit antiserum¹² (kindly provided by Yi-Shu Huang) for 1 hour at 4 °C, followed by biotinylated goat anti-rabbit IgG1 (Life Technologies) for 30 minutes. Cells were washed and stained with phycoerythrin (PE)-streptavidin (BD Biosciences) for 1 hour at 4 °C, washed again, and analyzed using an LSRII flow cytometer and Cell Quest Software (BD Biosciences).

Primary mast cell vibration and degranulation assays

To adhere cells, 96-well plates were coated with either 0.01% polylysine, 100 $\mu\text{g}/\text{mL}$ dermatan sulfate (chondroitin sulfate B), or 100 ng/mL anti-ADGRE2 antibody 2A1 in PBS for 5-6 hours at 37 $^{\circ}\text{C}$. Wells were washed with sterile PBS and 5000 cells were plated in each well. Plates were then centrifuged for 5 minutes at 450 g and incubated overnight. Adhered cells were washed and the medium was replaced with HEPES buffer with or without calcium chloride, and plates were vibrated at 750 rpm for 20 minutes on an orbital shaker. Release of β -hexosaminidase was measured as previously described¹³ and percent release was calculated. To quantitate the cells remaining attached after vibration in the presence or absence of calcium chloride, the ratio of β -hexosaminidase in cells that detached to total β -hexosaminidase was calculated. To quantitate the cells detached after vibration, the supernatant was collected and detached cells were counted.

Generation of expression constructs

Total RNA was isolated from patient blood preserved in PAXgene Blood RNA tubes using the Maxwell 16 LEV simplyRNA Blood Kit with the Maxwell 16 Instrument (Promega). AccuScribe high-fidelity reverse transcriptase (RT) (Agilent) was used to synthesize cDNA, and the open reading frame of *ADGRE2*, excluding the stop codon, was amplified using AccuPrime Pfx high-fidelity polymerase (Invitrogen) and a forward primer containing a CACC 5' overhang to allow directional TOPO cloning. Purified PCR product was inserted into the pENTR/D-TOPO entry vector (Invitrogen), and transformants were screened by PCR and Sanger sequencing. The GENEART Site-Directed Mutagenesis System (Invitrogen) was used on clones

of full-length splice variants to correct RT- or PCR-induced mutations, generate both nonmutated and p.C492Y mutated versions, and introduce the p.S518A cleavage-deficient mutation. Mutagenized clones were re-sequenced across the entire insert to ensure no off-target mutations were introduced during the mutagenesis PCR. A full-length error-free clone was used as the template for amplification of an N-terminal truncation mutant encoding amino acids 518-823 (NP_038475.2), with 6 base pairs encoding the amino acids methionine and alanine appended to the 5' end in order to provide a Kozak translation initiation sequence. This PCR product was also cloned into the pENTR/D-TOPO vector, as above.

The inserts from five constructs were transferred into the C-terminal Emerald Green Fluorescent Protein (EmGFP)-tagged Vivid Colors pcDNA6.2/C-EmGFP DEST Gateway destination vector (Invitrogen), using the Gateway LR Clonase II Enzyme Mix (Invitrogen). Validated clones plus the pcDNA6.2/C-EmGFP/GW/CAT control vector (expressing C-terminal EmGFP-tagged chloramphenicol acetyl transferase) were grown in 100 mL liquid cultures, and endotoxin-free plasmids were isolated using the EndoFree Plasmid Maxi Kit (Qiagen). The six final constructs were re-sequenced across the entire *ADGRE2-EmGFP* or *CAT-EmGFP* fused open reading frames to ensure fidelity during bacterial replication and a sequence match at all *ADGRE2* polymorphisms to the patient DNA sequence.

Transfection

Mature BMSCs were transfected using the Amaxa Nucleofector II (Lonza). Cells were centrifuged gently at 90 g for 10 minutes, washed once in PBS, and centrifuged again at 90 g for 10 minutes. BMSCs were then re-suspended in 100 μ L of transfection medium designed for the Amaxa system, containing 2 μ g of the appropriate construct. After transfection, 2×10^6 cells

were plated into 6-well plates with 2 mL of RPMI medium, and placed in a humidified incubator for 5 hours to recover. LAD2 cells were also transfected using the Amaxa Nucleofector II (Lonza), as described.¹⁴

Immunoblotting of transfected LAD2 cells

A 48-well plate was coated with 100 µg/mL of dermatan sulfate, and transfected LAD2 cells were adhered overnight. Cells were washed with HEPES buffer, lysed as previously described,¹⁵ and total protein was separated by electrophoresis on 4-12% NuPage Bis-Tris gels (Invitrogen). Blots were probed for immunoreactive proteins using monoclonal mouse anti-human ADGRE2 α subunit antibody, clone 2A1 (AbD Serotec), rabbit anti-GFP antibody (Sigma), and mouse anti-actin antibody (Sigma). Secondary detection was performed with infrared dye-labeled antibodies IRDye 680RD goat anti-mouse IgG (red) for ADGRE2 α subunit and actin, and IRDye 800CW donkey anti-rabbit IgG (green) for GFP-tagged ADGRE2 β subunit (LI-COR Biosciences). Two-color fluorescent imaging of infrared dyes was performed using the Odyssey CLx Imager (LI-COR Biosciences).

ADGRE2 adhesion to dermatan sulfate

Dermatan sulfate at different concentrations was coated onto 96-well plates for 4 hours, and 50,000 transfected mouse bone marrow-derived mast cells (BMMCs) were loaded per well. Cells were allowed to attach for 3 hours. Nonadherent cells were washed off, and remaining attached cells were quantitated using fluorescent CyQuant Dye (Invitrogen), at 480 nm excitation and 520 nm emission.

ADGRE2 trafficking

Mature BMMCs were transfected and assayed by flow cytometry for both surface trafficking of the ADGRE2 α subunit, as described above, and total expression of GFP-tagged ADGRE2 β subunit or CAT-GFP. Nonviable and doublet cells were excluded from the analysis.

ADGRE2 α and β subunit colocalization

Mature BMMCs were transfected as described above, and incubated for 5 hours to allow expression of transfected constructs. Cells were then plated into 8-well chambered coverglass coated with dermatan sulfate and allowed to adhere for 3 hours. The chambered coverglass was then either vibrated at 750 rpm for 20 minutes, or not vibrated. Supernatant was removed and adherent cells were placed on ice and washed with PBS. Cells were fixed in 4% paraformaldehyde for 30 minutes on ice, washed in PBS, and permeabilized in PBS containing 0.1% Triton X-100 and 1% BSA for 1 hour on ice. Fluorescent detection of GFP was performed as previously described,¹⁶ and immunostaining for the ADGRE2 α subunit was performed as described for flow cytometry, except that the streptavidin was conjugated with Alexa Fluor 568, which is more photostable than PE. After washing, 80% glycerol was added to the wells, and cells were visualized by confocal microscopy in the Biological Imaging Section of the Research Technologies Branch, NIAID, NIH, on a Leica TCS SP8 confocal microscope, as previously described.¹⁶ Image stacks through the depth of the cells were acquired (200 nm apart) to analyze the entire cell volumes, and sequential images were superimposed to eliminate cross-talk between fluorescent channels. Some intracellular nonspecific staining was observed with the control construct, but no evidence of plasma membrane staining was observed in the controls. Therefore, to eliminate the effect of nonspecific cytoplasmic staining, a mask was applied to the

GFP channel so that only GFP-positive voxels were analyzed for colocalization. As previously described,¹⁶ Imaris software was used for colocalization analyses using automatic thresholding after the mask was applied. The Pearson's coefficient in the colocalized volume was calculated, which measures the correlation between α and β subunit location and intensity.

Degranulation of LAD2 cells

After transfection, cells were plated in supplemented StemPro-34 medium containing rSCF¹⁰ to allow protein expression. For vibration-dependent degranulation assays, after 5 hours, 5×10^4 transfected LAD2 cells were transferred to triplicate wells of a flat bottom 96-well plate pre-coated with 100 $\mu\text{g}/\text{mL}$ dermatan sulfate, and incubated for an additional 3 hours at 37 °C to allow cell adhesion. Nonadherent cells were removed, and pre-warmed (37 °C) HEPES buffer was added to the wells. The plates were shaken on an orbital shaker at 750 rpm in an incubator at 37 °C for 20 minutes. Cells were cooled to 4 °C and centrifuged at 200 g for 5 minutes at 4 °C. Supernatants and pellets were assayed for β -hexosaminidase content, as described.¹⁴

To measure constitutive degranulation during the development of protein expression, 10^5 transfected LAD2 cells were removed from each transfection after 2 hours in rSCF, washed in pre-warmed HEPES buffer, and 10^4 cells per well were plated into duplicate wells of an untreated 96-well plate. Expression of the exogenous protein was first detectable 2 hours after transfection. Cells were incubated for an additional 3 hours at 37 °C while protein expression further developed, then cooled to 4 °C and centrifuged at 200 g for 5 minutes at 4 °C. Supernatants and pellets were assayed for β -hexosaminidase content, as above.

After cells were plated out for the degranulation assays, remaining cells were placed on ice and analysis of transfection efficiency and viability was performed using flow cytometry

(FacsCalibur). A subset of cells from each transfection was fixed with 4% paraformaldehyde in PBS for 30 minutes on ice, washed in PBS, and plated into chambered coverglass in 50% glycerol for later confocal imaging. Confocal microscopy was performed in the Biological Imaging Section of the Research Technologies Branch, NIAID, NIH, on a Leica TCS SP8 microscope. Images were collected using a 63X oil immersion objective NA 1.4. EmGFP was excited using an argon laser at 488 nm and data were collected with an HyD detector. Sequential images at 200 nm intervals were collected through the depth of the cells. Image snapshots were taken using Imaris software. Statistical significance of pairwise comparisons of different clones was assessed using ANOVA with Tukey's post-hoc test for multiple hypothesis correction.

II. Supplementary Figures

Figure S1. Serum tryptase levels in response to vibration

Serial serum tryptase measurements following forearm vortex challenge showed no significant change in either patients or a control, consistent with other physical urticarias. Dotted line indicates upper limit of reference range for control subjects (11.5 ng/mL). Tryptase levels were higher in patients than the control, but within normal limits. BL, baseline (prechallenge level).

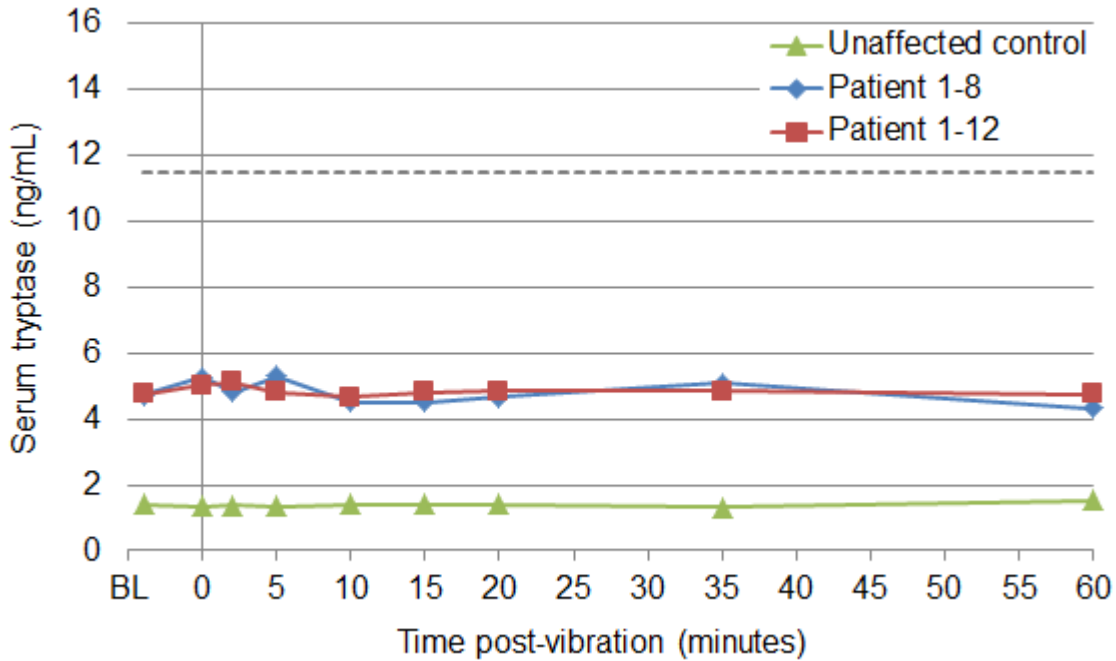


Figure S2. Candidate interval on chromosome 19p13 defined by linkage scans

In Family 1, a 6.4-Mb interval on chromosome 19p13, from rs12610201 to rs7259026, reached the maximum possible LOD score of 2.107 (top). In Family 2, a linkage scan at Yale University independently established linkage to the same region of chromosome 19p13. A subsequent scan using the same high-density SNP panel used for Family 1 showed that a 2.2-Mb region on chromosome 19p13, from rs809741 to rs4808027, reached the maximum possible LOD score of 5.117 (bottom). In both families, the remainder of the genome did not show linkage. Within the region of overlap represented by the Family 2 interval, the two families shared the same disease allele-bearing haplotype across 166 consecutive informative SNPs, spanning 1.7 Mb from rs11665898 to rs10421355. These data suggest that both families inherited the same pathogenic variant from an unknown common ancestor. Gray lines indicate LOD = 3.0 and LOD = -2.0.

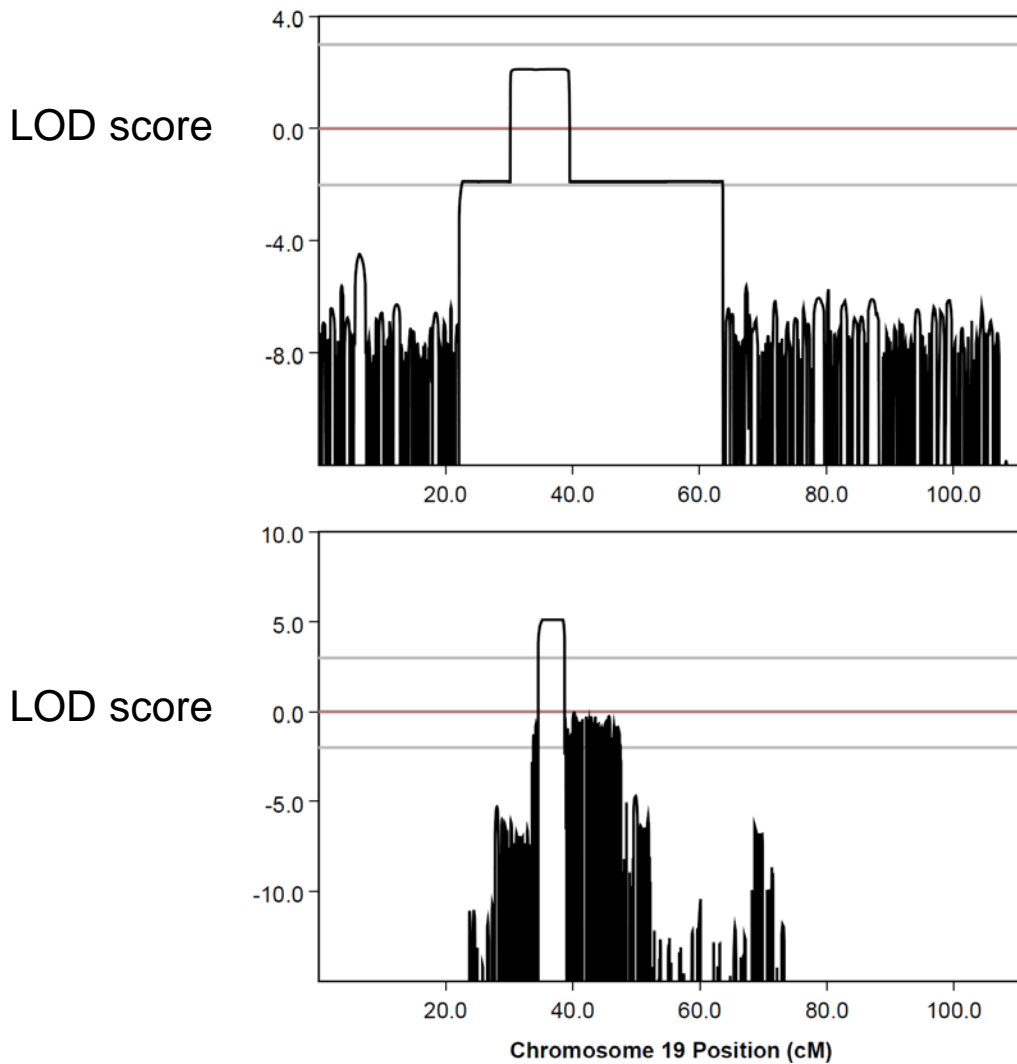
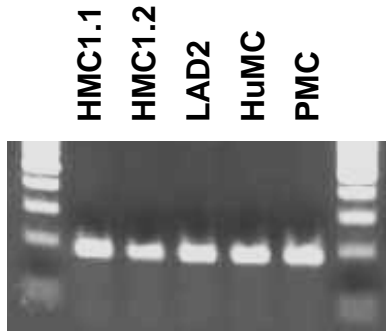
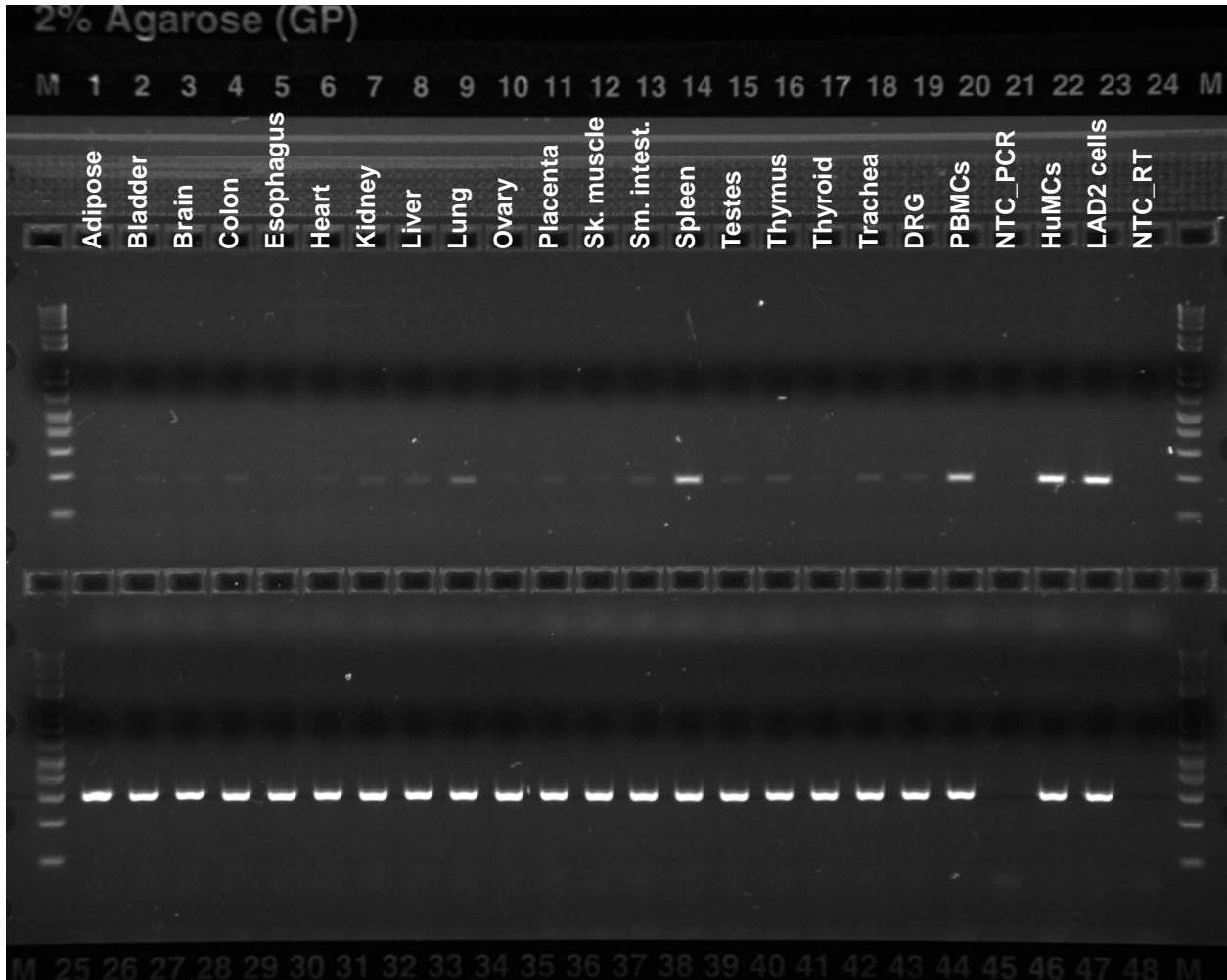


Figure S3. Expression of ADGRE2 in mast cells

A) *ADGRE2* mRNA is detectable in HMC1.1, HMC1.2, and LAD2 human mast cell lines, as well as stock human primary mast cell (HuMC) and fresh human primary mast cell (PMC) populations, as surveyed by RT-PCR.



B) *ADGRE2* mRNA (top row) is detectable in all human tissues surveyed by cycle-limited RT-PCR, but is most robustly expressed in primary human mast cells (HuMCs) and the LAD2 human mast cell line, with the next-highest expression in peripheral blood mononuclear cells (PBMCs) and spleen, compared to uniform ubiquitous expression of the housekeeping gene *RPLP0* (bottom row). DRG, dorsal root ganglion; NTC_PCR, no-template control for PCR reaction (water used in place of cDNA); NTC_RT, no-template control for reverse transcription (water used in place of RNA, and this mock RT reaction used as template for PCR).



C) Surface ADGRE2 protein expression is robust in three human mast cell lines (top) and two primary human mast cell populations (bottom) surveyed by flow cytometry using the 2A1 antibody. Total ADGRE2 protein expression from permeabilized cells shows a similar pattern (data not shown). Dotted line, isotype control; solid line, ADGRE2.

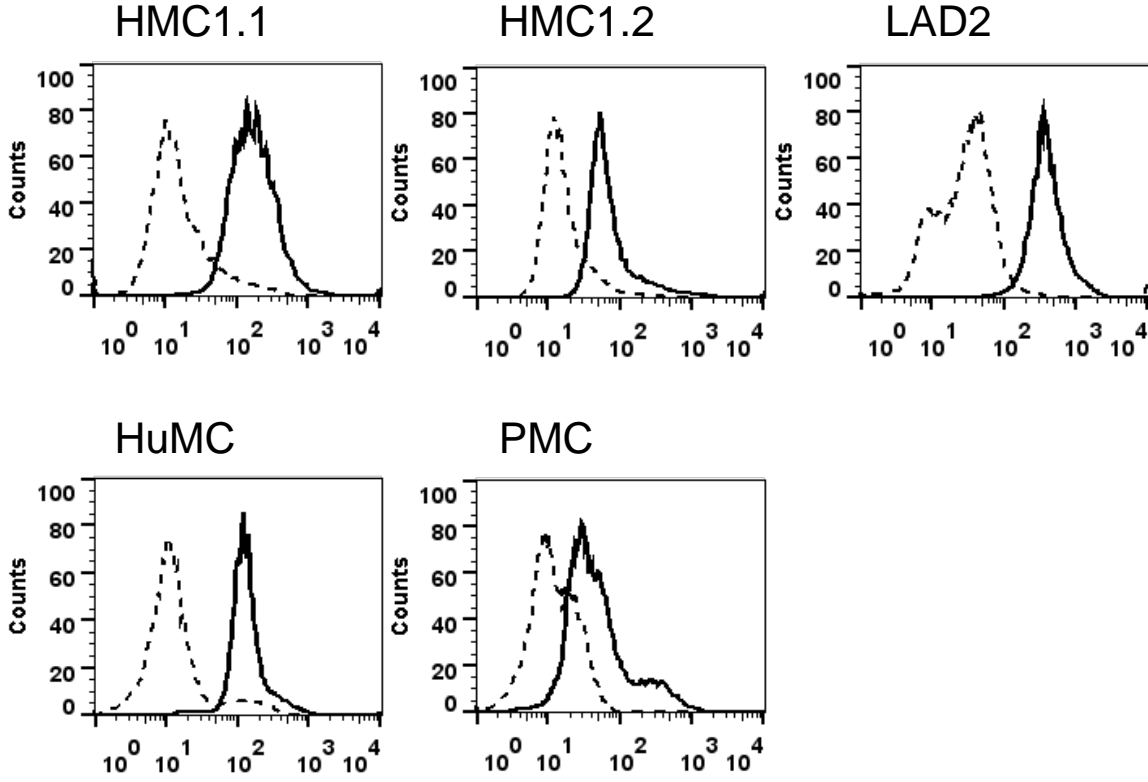
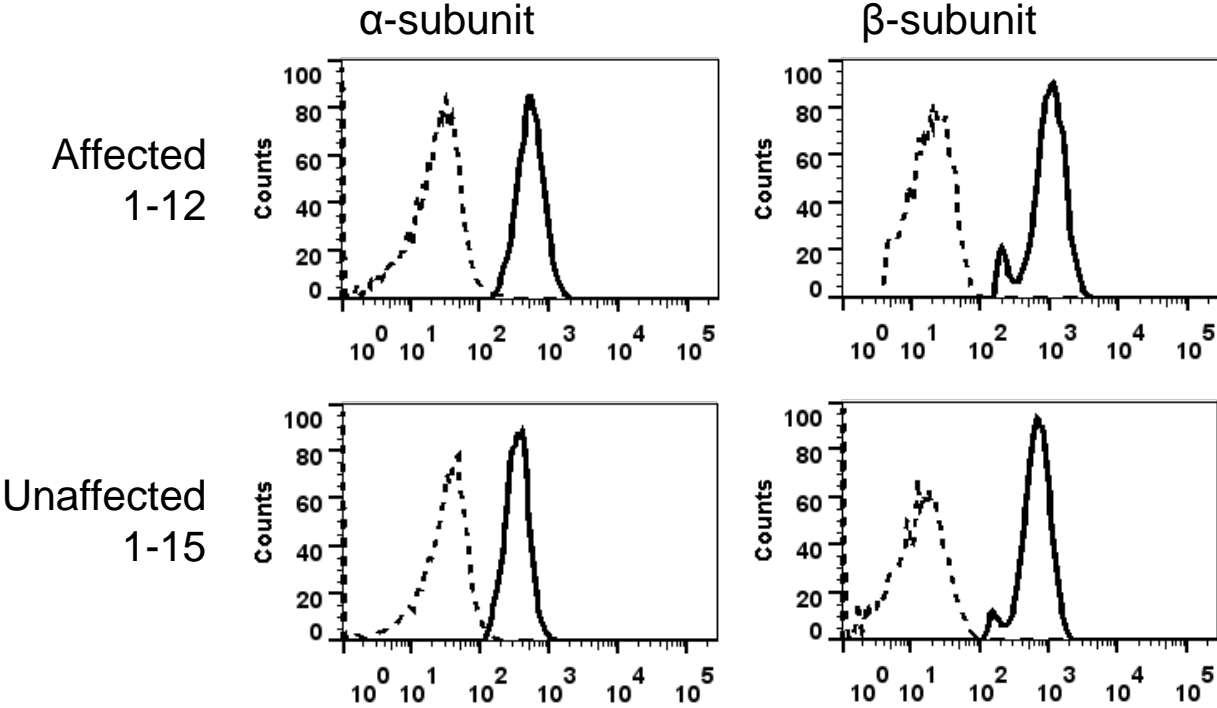
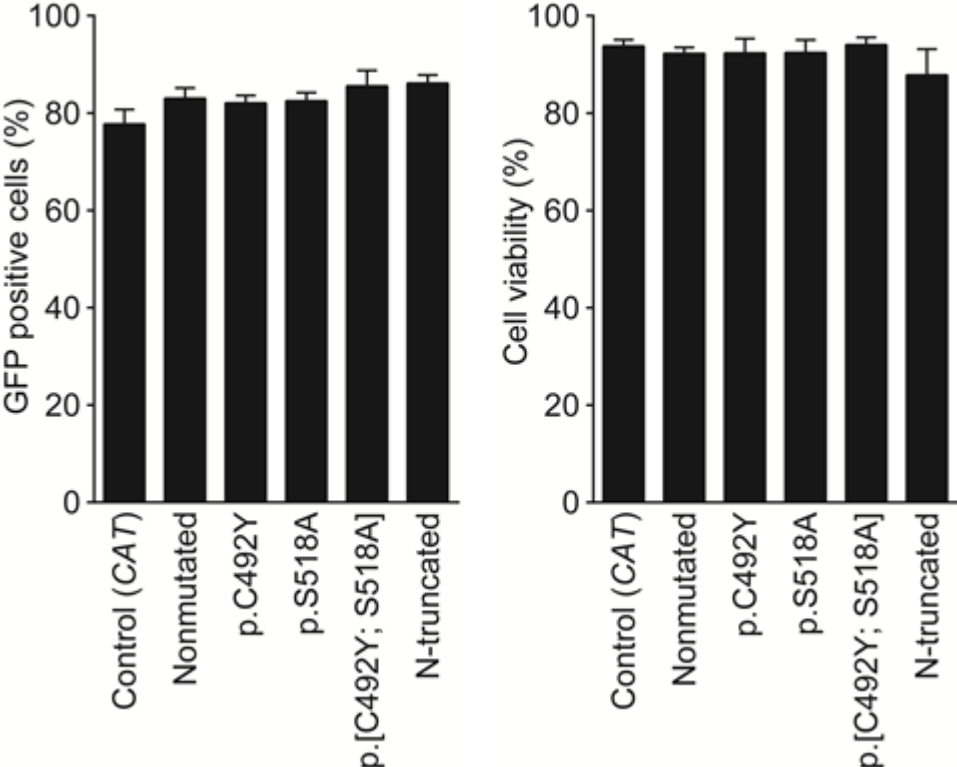


Figure S4. Expression, cleavage, adhesion, and trafficking of mutant ADGRE2

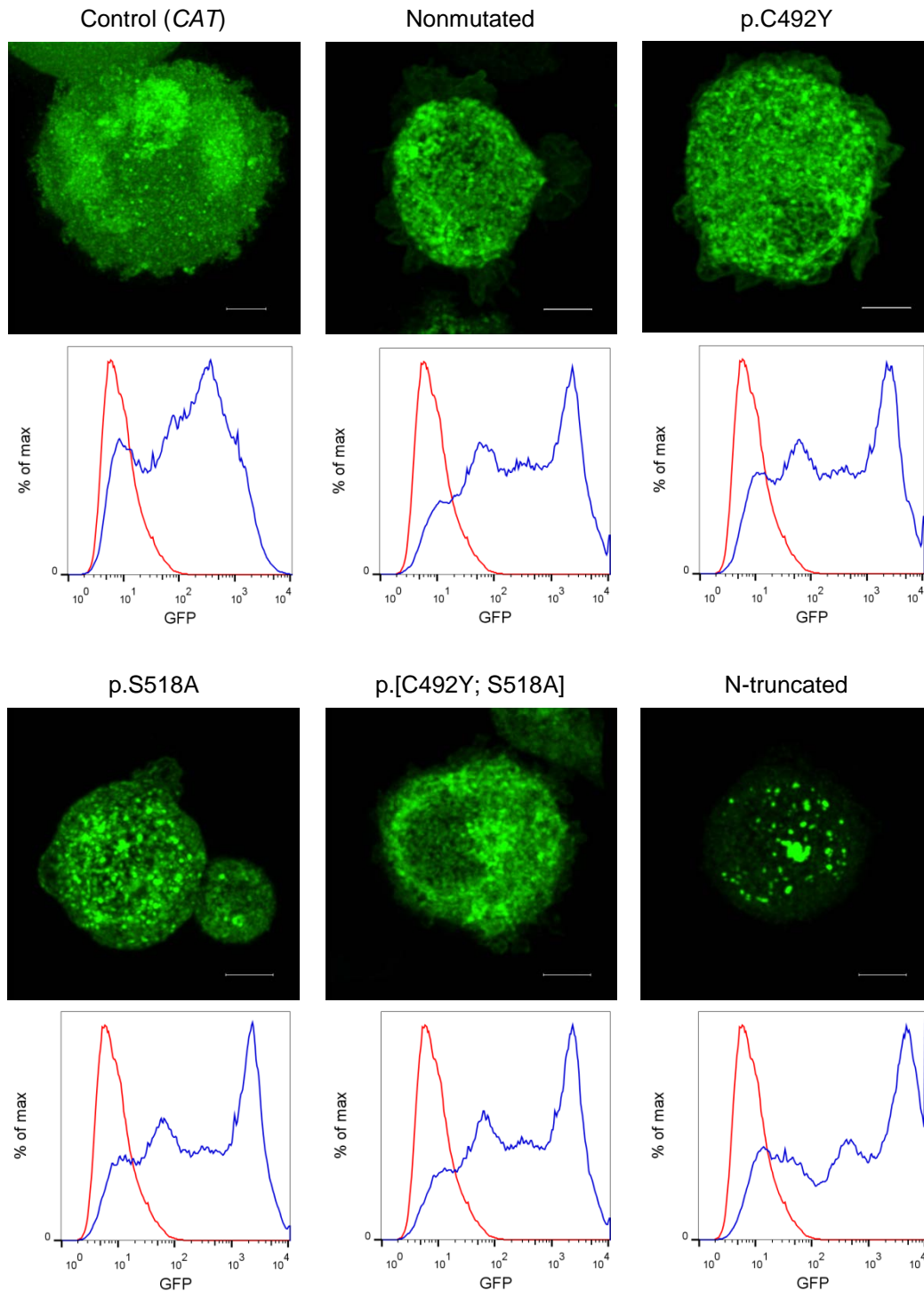
A) Flow cytometry of total ADGRE2 expression using antibodies to both subunits shows no difference in the relative expression of either subunit in patient vs. control PMCs. Dotted line, isotype control; solid line, ADGRE2.



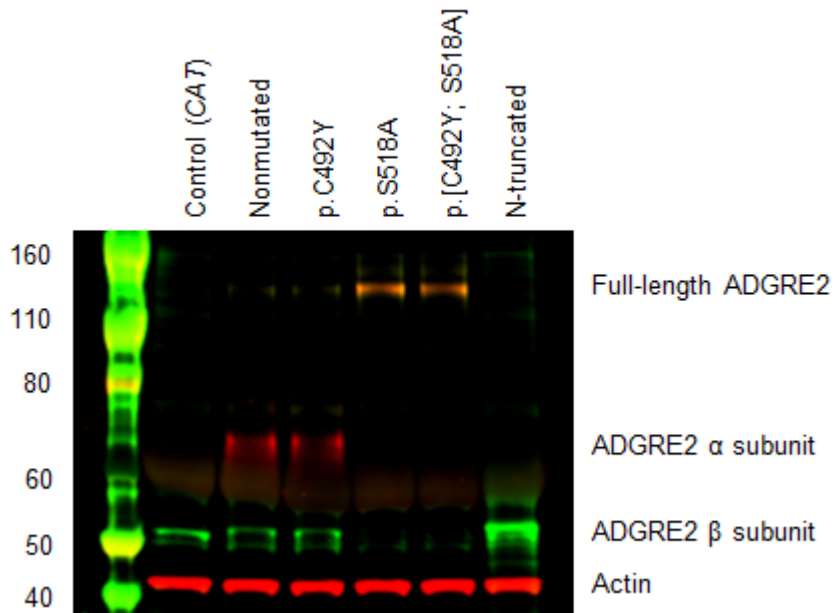
B) Transfection efficiency (left) and viability (right) for all six clones was uniformly high.



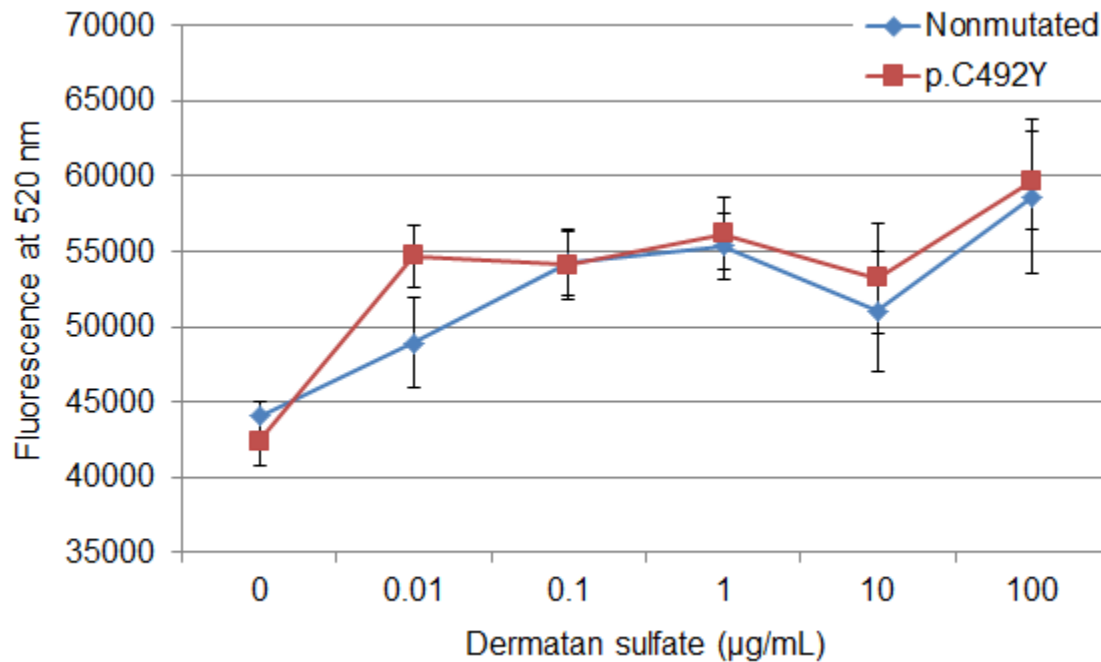
C) Composite Z-stacks of confocal micrographs of EmGFP expression in transfected LAD2 cells, with corresponding histograms. The control vector expresses a chloramphenicol acetyl transferase (*CAT*)-EmGFP fusion gene. The N-truncated mutant shows punctate cytoplasmic staining consistent with endocytic vesicles, suggesting the protein has been internalized. Red line, no cDNA mock-transfected control; blue line, transfected. Scale bars 5 μ m.



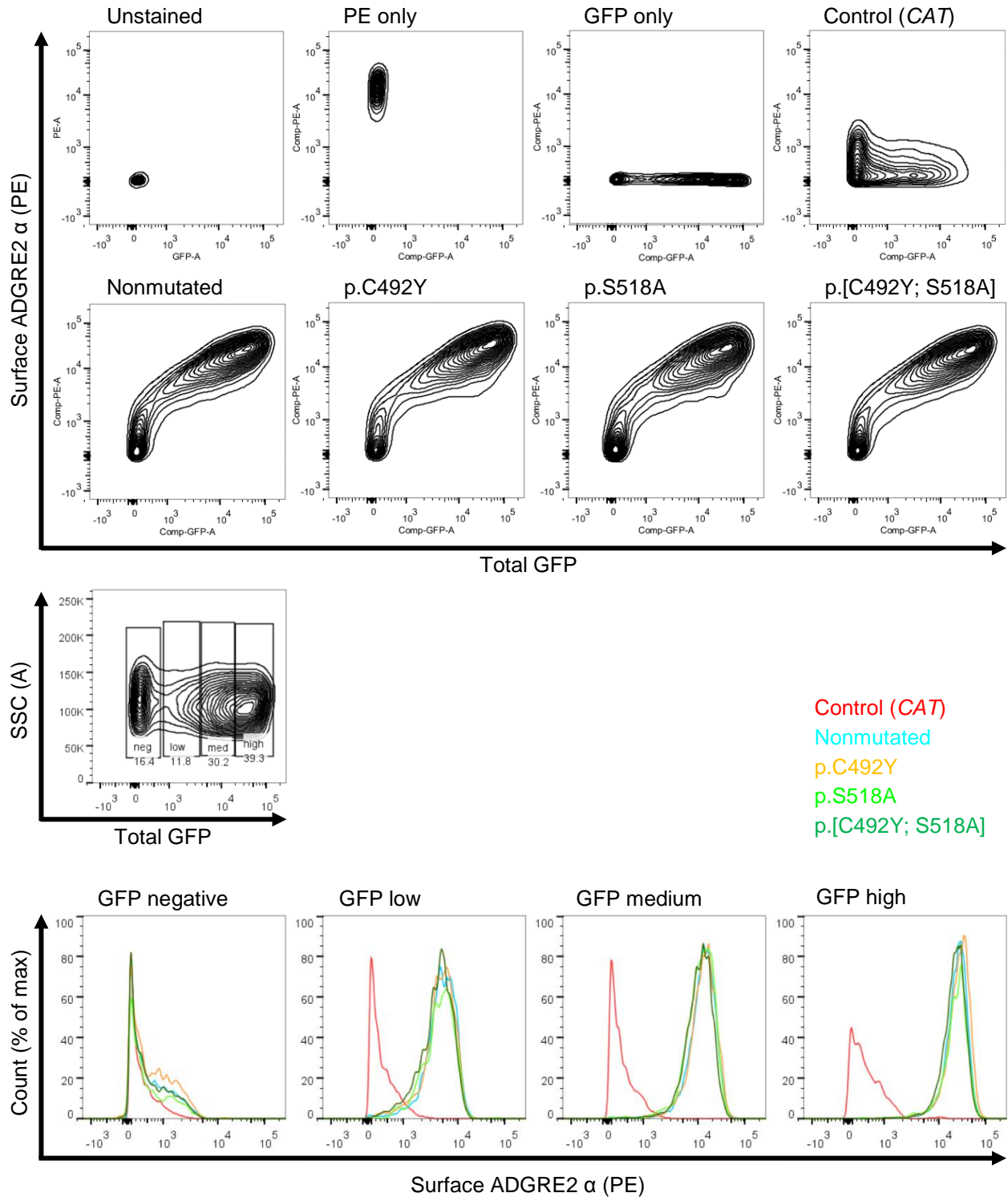
D) Immunoblotting of transfected LAD2 cells with infrared two-color detection, using an anti-ADGRE2 α subunit antibody (red) and an anti-GFP antibody (green) that labels the β subunit, revealed no difference in cleavage between nonmutated and p.C492Y *ADGRE2*, and confirmed lack of cleavage of p.S518A and p.[C492Y; S518A] cleavage-deficient mutants. The control vector expresses a chloramphenicol acetyl transferase (*CAT*)-EmGFP fusion gene, encoding a product with a predicted 54 kDa molecular weight. Yellow indicates overlap of red and green signal. Kilodalton sizes of the molecular ladder markers are indicated to the left.



E) Transfected murine bone marrow-derived mast cells (BMMCs) were allowed to adhere to plates coated with a range of dermatan sulfate concentrations, and adherent cells were quantitated. There is no mouse orthologue for *ADGRE2*, so adhesion is not affected by endogenous protein. Data represent means \pm SEM for three parallel experiments, each measured in duplicate.



F) Surface expression of phycoerythrin (PE)-labeled ADGRE2 α subunit and total expression of GFP-tagged β subunit or CAT-GFP in transfected BMBCs was measured by flow cytometry (top two rows). Gating on GFP expression levels (third row), the number of surface α subunit-positive cells for the five expression clones was counted (bottom row).



III. Supplementary Tables

Table S1. Variant databases in which *ADGRE2*:c.1475G>A is absent

dbSNP v146*
77,238 exomes and genomes from the Kaviar database (September 2015 release)*
60,706 exomes from the Exome Aggregation Consortium (v0.3)
32,488 exomes from the Haplotype Reference Consortium
6,503 exomes from the NHLBI Exome Sequencing Project
2,577 genomes from the 1000 Genomes Project (August 2015 release)
662 exomes from the NHGRI ClinSeq project*
95 exomes from the NIEHS Environmental Genome Project
69 public genomes sequenced at Complete Genomics, Inc.

Databases are not independent. NHLBI, National Heart, Lung, and Blood Institute; NHGRI, National Human Genome Research Institute; NIEHS, National Institute of Environmental Health Sciences.

*The proband from Family 1 was sequenced in the NHGRI ClinSeq project and her *ADGRE2* variant was detected; accordingly, a single variant allele is present in the ClinSeq database, as well as in dbSNP v137 and above (into which the ClinSeq data were deposited) and Kaviar (into which dbSNP was deposited).

Table S2. Physical urticaria patients screened for *ADGRE2* variants

Diagnosis	Number of subjects
Vibratory urticaria	10
Dermatographism	8
Delayed pressure urticaria	4
Cold urticaria	22
Cholinergic urticaria	11
Local heat-induced urticaria	3
Solar urticaria	2

The 60 screened patients were unrelated to each other and to Families 1-3.

Table S3. Pairwise *P* values for constitutive degranulation of LAD2 cells

Statistical significance for Fig. 3C was determined using one-way ANOVA with Tukey's post-hoc test for multiple hypothesis correction. CI, confidence interval of mean difference.

* $P < 0.05$, ** $P < 0.01$.

Comparison	Mean difference	95% CI	Significance
Control (<i>CAT</i>) vs. nonmutated	-2.167	-11.80 to 7.469	
Control (<i>CAT</i>) vs. p.C492Y	-2.435	-12.07 to 7.201	
Control (<i>CAT</i>) vs. p.S518A	-1.867	-11.50 to 7.769	
Control (<i>CAT</i>) vs. p.[C492Y; S518A]	-3.814	-13.45 to 5.821	
Control (<i>CAT</i>) vs. N-truncated	-12.26	-21.89 to -2.623	**
Nonmutated vs. p.C492Y	-0.2682	-9.904 to 9.367	
Nonmutated vs. p.S518A	0.3001	-9.336 to 9.936	
Nonmutated vs. p.[C492Y; S518A]	-1.648	-11.28 to 7.988	
Nonmutated vs. N-truncated	-10.09	-19.73 to -0.4559	*
p.C492Y vs. p.S518A	0.5683	-9.067 to 10.20	
p.C492Y vs. p.[C492Y; S518A]	-1.379	-11.02 to 8.256	
p.C492Y vs. N-truncated	-9.823	-19.46 to -0.1876	*
p.S518A vs. p.[C492Y; S518A]	-1.948	-11.58 to 7.688	
p.S518A vs. N-truncated	-10.39	-20.03 to -0.7560	*
p.[C492Y; S518A] vs. N-truncated	-8.444	-18.08 to 1.192	

Table S4. Pairwise *P* values for vibration-induced degranulation of LAD2 cells

Statistical significance for Fig. 3D was determined using two-way repeated measures ANOVA with Tukey's post-hoc test for multiple hypothesis correction. CI, confidence interval of mean difference. **P*<0.05, ***P*<0.01, ****P*<0.001, *****P*<0.0001.

Comparison	Mean difference	95% CI	Significance
Nonvibrated			
Control (<i>CAT</i>) vs. nonmutated	-1.357	-5.670 to 2.957	
Control (<i>CAT</i>) vs. p.C492Y	-1.958	-6.272 to 2.355	
Control (<i>CAT</i>) vs. p.S518A	-1.252	-5.566 to 3.061	
Control (<i>CAT</i>) vs. p.[C492Y; S518A]	-2.283	-6.597 to 2.031	
Control (<i>CAT</i>) vs. N-truncated	-4.014	-8.328 to 0.2993	
Nonmutated vs. p.C492Y	-0.6018	-4.915 to 3.712	
Nonmutated vs. p.S518A	0.1043	-4.209 to 4.418	
Nonmutated vs. p.[C492Y; S518A]	-0.9263	-5.240 to 3.387	
Nonmutated vs. N-truncated	-2.658	-6.971 to 1.656	
p.C492Y vs. p.S518A	0.7061	-3.608 to 5.020	
p.C492Y vs. p.[C492Y; S518A]	-0.3245	-4.638 to 3.989	
p.C492Y vs. N-truncated	-2.056	-6.369 to 2.258	
p.S518A vs. p.[C492Y; S518A]	-1.031	-5.344 to 3.283	
p.S518A vs. N-truncated	-2.762	-7.076 to 1.552	
p.[C492Y; S518A] vs. N-truncated	-1.731	-6.045 to 2.582	
Vibrated			
Control (<i>CAT</i>) vs. nonmutated	-5.251	-9.565 to -0.9379	*
Control (<i>CAT</i>) vs. p.C492Y	-11.47	-15.78 to -7.155	****
Control (<i>CAT</i>) vs. p.S518A	-2.599	-6.913 to 1.715	
Control (<i>CAT</i>) vs. p.[C492Y; S518A]	-3.24	-7.554 to 1.073	
Control (<i>CAT</i>) vs. N-truncated	-5.421	-9.735 to -1.108	*
Nonmutated vs. p.C492Y	-6.217	-10.53 to -1.903	**
Nonmutated vs. p.S518A	2.652	-1.661 to 6.966	
Nonmutated vs. p.[C492Y; S518A]	2.011	-2.302 to 6.325	
Nonmutated vs. N-truncated	-0.1696	-4.483 to 4.144	
p.C492Y vs. p.S518A	8.869	4.556 to 13.18	****
p.C492Y vs. p.[C492Y; S518A]	8.228	3.914 to 12.54	***
p.C492Y vs. N-truncated	6.047	1.734 to 10.36	**
p.S518A vs. p.[C492Y; S518A]	-0.6412	-4.955 to 3.672	
p.S518A vs. N-truncated	-2.822	-7.136 to 1.492	
p.[C492Y; S518A] vs. N-truncated	-2.181	-6.494 to 2.133	

IV. Supplementary References

1. Epstein PA, Kidd KK. Dermo-distortive urticaria: an autosomal dominant dermatologic disorder. *Am J Med Genet* 1981;9:307-15.
2. Abecasis GR, Cherny SS, Cookson WO, Cardon LR. Merlin--rapid analysis of dense genetic maps using sparse gene flow trees. *Nat Genet* 2002;30:97-101.
3. DePristo MA, Banks E, Poplin R, et al. A framework for variation discovery and genotyping using next-generation DNA sequencing data. *Nat Genet* 2011;43:491-8.
4. Wang K, Li M, Hakonarson H. ANNOVAR: functional annotation of genetic variants from high-throughput sequencing data. *Nucleic Acids Res* 2010;38:e164.
5. Quinlan AR, Hall IM. BEDTools: a flexible suite of utilities for comparing genomic features. *Bioinformatics* 2010;26:841-2.
6. Robinson JT, Thorvaldsdottir H, Winckler W, et al. Integrative genomics viewer. *Nat Biotechnol* 2011;29:24-6.
7. Kirshenbaum AS, Metcalfe DD. Growth of human mast cells from bone marrow and peripheral blood-derived CD34+ pluripotent progenitor cells. *Methods Mol Biol* 2006;315:105-12.
8. Jensen BM, Swindle EJ, Iwaki S, Gilfillan AM. Generation, isolation, and maintenance of rodent mast cells and mast cell lines. *Curr Protoc Immunol* 2006;Chapter 3:Unit 3 23.
9. Radinger M, Jensen BM, Kuehn HS, Kirshenbaum A, Gilfillan AM. Generation, isolation, and maintenance of human mast cells and mast cell lines derived from peripheral blood or cord blood. *Curr Protoc Immunol* 2010;Chapter 7:Unit 7 37.
10. Kirshenbaum AS, Akin C, Wu Y, et al. Characterization of novel stem cell factor responsive human mast cell lines LAD 1 and 2 established from a patient with mast cell sarcoma/leukemia; activation following aggregation of FcepsilonRI or FcgammaRI. *Leuk Res* 2003;27:677-82.
11. Kwakkenbos MJ, Chang GW, Lin HH, et al. The human EGF-TM7 family member EMR2 is a heterodimeric receptor expressed on myeloid cells. *J Leukoc Biol* 2002;71:854-62.
12. Huang YS, Chiang NY, Hu CH, et al. Activation of myeloid cell-specific adhesion class G protein-coupled receptor EMR2 via ligation-induced translocation and interaction of receptor subunits in lipid raft microdomains. *Mol Cell Biol* 2012;32:1408-20.
13. Kuehn HS, Radinger M, Gilfillan AM. Measuring mast cell mediator release. *Curr Protoc Immunol* 2010;Chapter 7:Unit7 38.
14. Cruse G, Beaven MA, Ashmole I, Bradding P, Gilfillan AM, Metcalfe DD. A truncated splice-variant of the FcepsilonRIbeta receptor subunit is critical for microtubule formation and degranulation in mast cells. *Immunity* 2013;38:906-17.
15. Tkaczyk C, Metcalfe DD, Gilfillan AM. Determination of protein phosphorylation in Fc epsilon RI-activated human mast cells by immunoblot analysis requires protein extraction under denaturing conditions. *J Immunol Methods* 2002;268:239-43.
16. Cruse G, Beaven MA, Music SC, Bradding P, Gilfillan AM, Metcalfe DD. The CD20 homologue MS4A4 directs trafficking of KIT toward clathrin-independent endocytosis pathways and thus regulates receptor signaling and recycling. *Mol Biol Cell* 2015;26:1711-27.